

Precipitation of Iron on the Surface of *Leptospira interrogans* Is Associated with Mutation of the Stress Response Metalloprotease HtpX

Rebekah Henry,^{a,*} Miranda Lo,^{a,d} Chenai Khoo,^{a,d} Hailong Zhang,^c Reinhard I. Boysen,^c Mathieu Picardeau,^b Gerald L. Murray,^a Dieter M. Bulach,^{a,e} Ben Adler^{a,d}

Department of Microbiology, Monash University, Clayton, Victoria, Australia^a; Institut Pasteur, Unité de Biologie des Spirochètes, Paris, France^b; Australian Research Council Special Research Centre for Green Chemistry, Monash University, Clayton, Victoria, Australia^c; Australian Research Council Centre of Excellence in Structural and Functional Microbial Genomics, Monash University, Clayton, Victoria, Australia^d; Victorian Bioinformatics Consortium, Monash University, Clayton, Victoria, Australia^e

High concentrations of free metal ions in the environment can be detrimental to bacterial survival. However, bacteria utilize strategies, including the activation of stress response pathways and immobilizing chemical elements on their surface, to limit this toxicity. In this study, we characterized LA4131, the HtpX-like M48 metalloprotease from *Leptospira interrogans*, with a putative role in bacterial stress response and membrane homeostasis. Growth of the *la4131* transposon mutant strain (L522) in 360 μM FeSO_4 (10-fold the normal *in vitro* concentration) resulted in the production of an amorphous iron precipitate. Atomic force microscopy and transmission electron microscopy analysis of the strain demonstrated that precipitate production was associated with the generation and release of outer membrane vesicles (OMVs) from the leptospiral surface. Transcriptional studies indicated that inactivation of *la4131* resulted in altered expression of a subset of metal toxicity and stress response genes. Combining these findings, this report describes OMV production in response to environmental stressors and associates OMV production with the *in vitro* activity of an HtpX-like metalloprotease.

Iron is a highly abundant, redox-reactive metal. The redox chemistry of iron allows it to readily transition between Fe (II) and Fe (III) states. This property, combined with its abundance, makes iron a key metal in environmental microbe-metal interactions (1). In order to manage their environment, bacteria have developed the capacity to associate with and precipitate metal ions from aqueous sources (2, 3). Extracellular biogenic iron oxides are amorphous iron precipitates closely associated with cell walls and exopolymers of bacteria and are the most common extracellular metal species affiliated with microorganisms (4, 5). The precipitation of iron on the surface of bacteria resulting in the formation of amorphous iron oxides occurs by both active and passive processes (5).

Active formation of iron precipitates can result from metabolic processes, whereby metabolic byproducts oxidize the metal ions, causing the formation of amorphous minerals (6). An example of active metal ion precipitation is the selective regulation of iron oxyhydroxide formation on the surface of the neutrophilic, Fe (II)-oxidizing bacteria of the genus *Leptothrix* (6, 7). Although the metabolic pathways involved in this process have not been fully characterized, regulation of iron oxidation by *Leptothrix* may enhance metabolic energy generation under certain environmental conditions (5).

Passive iron oxide formation is the result of structures at the bacterial surface facilitating the accumulation, nucleation, and precipitation of metal ions (5). Bacterial cell surfaces most commonly have an overall net negative charge resulting from the presence of cell wall components such as polysaccharides (5). Electrostatic interaction between positively charged metal ions and the negatively charged bacterial surface can result in metal adsorption (3, 5). Nucleation and precipitation of adsorbed Fe (III) occur when localized concentrations are sufficiently high at surface reactive sites (5). Precipitates become stabilized at the bacterial sur-

face and serve as sites for further metal aggregation (3). Under extreme conditions, visible flocs of precipitated iron oxyhydroxide can be formed, leading to destabilized outer membranes (OM) and outer membrane vesicle (OMV) formation (2).

Bacteria do not gain any metabolic advantage from passive nucleation events. Instead, it is thought that passive iron oxide formation may represent a survival mechanism to prevent cell death by decreasing the concentration of iron in solution to non-toxic levels (5). Thus, passive nucleation, metal precipitation, and OMV formation represent a putative stress-response mechanism for heavy metal resistance (3).

Outer membrane vesicles are membranous structures derived from the OM of Gram-negative bacteria. Vesiculation is a ubiquitous process, occurring in both pathogenic and saprophytic organisms during normal growth (8–11). OMVs are primarily composed of soluble periplasmic proteins encased within an OM sheath (8). Roles for OMVs in bacterial pathogenesis have been previously described (12–17). However, functions associated with bacterial survival remain unclear. To date, only a role in environmental stress response has been demonstrated.

Bacterial stress responses can be defined as “a cascade of alterations in gene expression and protein activity for the purpose of surviving extreme and rapidly changing and potentially dam-

Received 4 April 2013 Accepted 22 May 2013

Published ahead of print 24 May 2013

Address correspondence to Ben Adler, Ben.Adler@monash.edu.

* Present address: Rebekah Henry, Department of Civil Engineering, Monash University, Clayton, Victoria, Australia.

Copyright © 2013, American Society for Microbiology. All Rights Reserved.

doi:10.1128/AEM.01097-13

TABLE 1 Database sources for comparative sequence analysis

Gene	Species/strain	GenBank accession no.	Reference
<i>la4131</i>	<i>L. interrogans</i> sv Lai	AAN51329	48
<i>htpX</i>	<i>E. coli</i>	AAA62779	62
<i>lic13293</i>	<i>L. interrogans</i> sv Copenhageni	AE016823	47
<i>lman3580</i>	<i>L. interrogans</i> sv Manilae	AHPU00000000	77
<i>lip0012</i>	<i>L. interrogans</i> sv Pomona	NZ_AFLT02000043	
	<i>L. biflexa</i> sv Patoc	CP000777	78
	<i>L. borgpetersenii</i> sv Hardjobovis	CP000348	66

aging conditions" (18). The σ^E proteolysis pathway (19) and Cpx two-component signal transduction system (20) are involved in envelope maintenance, adaptation, and protection in response to environmental stress (21–25). Both pathways regulate the expression and constitutive degradation of misfolded proteins within the cell periplasm. At high temperatures, the protease DegP is transcriptionally regulated by both systems to prevent the accumulation of toxic products (10, 26). Studies have demonstrated induction of OMV production, under high temperatures, in response to *degP* mutation and associated accumulation of misfolded proteins within the periplasm (8, 10, 26, 27). Multiple proteases, other than DegP, have been identified as key components in both Cpx and σ^E pathways. Transcription of proteases is regulated by a wide range of environmental stimuli, suggesting, in turn, that OMV production may be stimulated under a range of different conditions.

The *Escherichia coli* metalloprotease HtpX degrades accumulated and misfolded protein products in both the σ^E and Cpx pathways (21, 28, 29). Orthologs of HtpX are present in nearly all bacteria. Mutational inactivation of HtpX causes increased thermal sensitivity, growth retardation, abnormal protein translocation, accumulation of misfolded products, and altered surface adhesiveness, cellular morphology, and surface antigen expression (28–31). This suggests that HtpX plays a central role in maintaining the various functions of the outer membrane.

In this paper, we present a phenotypic analysis of a strain of *Leptospira interrogans* in which the gene encoding LA4131, an OM-associated HtpX-like metalloprotease, has been insertionally inactivated. In particular, we show that this strain is defective in the normal active processes used by *Leptospira* to manage high concentrations of extracellular soluble iron. Mass spectrometry (MS), atomic force microscopy (AFM), and transmission electron microscopy (TEM) analysis of the mutant demonstrated the production of an amorphous iron precipitate associated with the generation and release of OMVs from the leptospiral surface. Combined, these data indicate that passive nucleation stress-response processes are induced in direct response to inactivation of a HtpX-like metalloprotease. This report extends the repertoire of functions maintained by HtpX and adds to an existing body of work that shows that HtpX metalloproteases are essential for the normal function of the bacterial outer membrane.

MATERIALS AND METHODS

Bioinformatics analysis. The nucleotide and deduced amino acid sequences of *la4131* were obtained from GenBank (NP_714311) (Table 1). Identification of conserved domains was conducted with RPS-BLAST (<http://www.ncbi.nlm.nih.gov/Structure/cdd/wrpsb.cgi>). A cellular location for LA4131 was predicted using a combination of pSORTB (32, 33), SignalP (34), Lipop (35), SpLip (36), and SecretomeP (37, 38). Protein membrane topology was predicted using ConPredII (39).

Bacterial strains and culture conditions. Random transposon mutagenesis of *L. interrogans* serovar (sv) Lai strain L56601 (designated L521 in this study) was described previously (40). Disruption of *la4131* in mutant clone L56 (designated L522 in this study) was confirmed by direct sequencing from genomic DNA as described by Murray et al. (41). Leptospire were routinely cultured at 30°C in EMJH medium (Becton, Dickinson and Co., Sparks, MD) with kanamycin (50 µg/ml) where appropriate. Based on the observation of phenotypic variation in particular lots of medium, lots 701688 and 8170035 were selected for iron phenotype experiments. Supplementation with 360 µM FeSO₄ was used, where specified, for the cultivation of strains during iron precipitation investigations.

ICP-MS. Inductively coupled plasma mass spectrometry (ICP-MS) is a technique for quantification of analytes to subnanogram concentrations. Isotopic fingerprints display all constituent elemental isotopes at their respective atomic masses; each peak height represents the quantitative number (counts) of ions detected for each isotope (42). Four stable isotopes of iron (Fe⁵⁴, Fe⁵⁶, Fe⁵⁷, and Fe⁵⁸) (43) can be resolved by ICP-MS. Three replicate 50-ml cultures of L521 and L522 were cultivated at 30°C in EMJH medium with or without iron supplementation until a density of 1×10^9 cells/ml was reached. The cultures were pelleted and washed twice at $8,500 \times g$ for 15 min and resuspended in 10 ml of EMJH base solution (Becton, Dickinson and Co., Sparks, MD). The washed cell pellets were resuspended in 3 ml of 1% nitric acid to dissolve organic and inorganic cellular material. Inductively coupled plasma mass spectrometry was conducted at the Monash University School of Geosciences (Clayton, Victoria, Australia) (44).

Atomic force microscopy (AFM). Cultures of *L. interrogans* were grown to a density of 5×10^8 cells/ml in 5 ml of EMJH medium with or without iron supplementation. One milliliter of culture was removed and centrifuged at $5,000 \times g$ for 15 min. The culture supernatant was removed and the pellet carefully resuspended in 100 µl sterile deionized H₂O. The culture was pelleted at $5,000 \times g$ for 15 min, and the cells were resuspended in sterile deionized H₂O to a final density of 1×10^7 cells/ml. A 10-µl aliquot of the diluted cell suspension was air dried onto heat-treated glass microscope slides under aseptic conditions.

Surface characterization was undertaken in air with a PicoPlus atomic force microscope (AFM) interfaced with a Picoscan 3000 controller (Molecular Imaging Inc.). A silicon cantilever (Ultrasharp, NSC15/AIBS; MikroMasch) was used with a typical spring constant of 40 N/m in tapping and phase-contrast modes. The resulting images were analyzed using WSxM 4.0 Develop 11.6 software. AFM imaging was performed twice on independently prepared samples.

Transmission electron microscopy (TEM). Cultures of *L. interrogans* were grown in EMJH medium with or without iron supplementation, pelleted, and resuspended in sterile deionized H₂O to a final density of 1×10^7 cells/ml. Paired samples of cells were fixed onto Formvar/carbon-coated grids for 10 min and washed for 5 min with sterile deionized water. One grid from each pair was negatively stained with 2% phosphotungstic acid (pH 7.0) for 30 s to serve as a stained-image control. Samples were examined with a Hitachi H7500 electron microscope (Hitachi High Technologies America, Pleasanton, CA).

Microarray analysis. Three biological replicate RNA samples from *L. interrogans* sv Lai (L521) and the *L. interrogans* sv Lai *la4131* mutant (L522) were grown in 100 ml EMJH medium with or without iron supplementation. Cells were harvested at a density of between 4×10^8 and 7×10^8 cells/ml. RNA purification, reverse transcription, microarray construction, cDNA hybridization, and array image analysis were conducted as described previously (45). All conditions tested were cross-compared.

RESULTS

LA4131 is a putative outer membrane M48 metalloprotease. The *la4131* gene of *L. interrogans* sv Lai strain L56601 consists of 1,977 nucleotides, encoding a protein of 659 amino acids. The distribution of *la4131* in the genus *Leptospira* is unusual, with no ortholog identified in the genome of the bovine pathogen *L. borgpetersenii*

sv Hardjobovis L550 strain (GenBank accession no. CP000348). However, a protein sharing 28% similarity was identified in the saprophyte *L. biflexa* sv Patoc Patoc1 strain (GenBank accession no. CP000777). Orthologs were also identified in isolates from the pathogenic species *L. interrogans*, *L. kirschneri*, *L. kmetyi*, and *L. noguchii* as well as intermediate species *L. inadai*, *L. broomii*, and *L. licerasiae* (47–49).

RPS-BLAST analysis indicated that LA4131 contains an M48 superfamily domain (pfam01435) between residues 75 and 264; this M48 domain has a conserved zinc-binding motif, HELSH, between residues 143 and 147. These features are consistent with the identification of LA4131 as a putative bacterial metalloprotease. Analysis of the peptide sequence using SpLip, LipoP, and SignalP predicted that LA4131 has a leader sequence with a signal peptidase 1 cleavage site between residues 22 and 23. Thus, LA4131 is predicted to be localized in the OM. Beta strands and coiled regions were predicted at the C-terminal end of the protein after residue 530, further supporting an OM localization (50).

Inactivation of *la4131* results in growth medium-dependent iron precipitate production. Strain L522 was derived from *L. interrogans* sv Lai strain L56601 (40). The transposon inserted at nucleotide 178 of the coding region of *la4131*. Quantitative reverse transcription-PCR (qRT-PCR) comparisons between the parent L521 strain and mutant L522 measured an 8-fold reduction ($P < 0.01$) in transcript levels after the point of transposon insertion in *la4131* (data not shown).

No difference between the parent and mutant strains in growth rates was observed after routine culture in EMJH medium. However, with EMJH medium containing a high level of iron (360 μM FeSO_4), phenotypic differences between L522 and the parental strain (L521) were observed; an orange precipitate formed in cultures of the *la4131* mutant (L522) but not in those of the parent (L521). The formation of this precipitate was associated with an increase in cell pellet size; when 1 ml of culture (standardized for cell density) was centrifuged, the cell pellet sizes ranged from 100 μl to 250 μl . The wild-type (WT) strain consistently produced a pellet of 100 μl (Fig. 1A). We were alerted to the phenotype of L522 during routine culture in EMJH medium, with some cultures forming the orange precipitate. In EMJH medium not producing a phenotypic difference, such as lot 8170035, supplementing the medium with a final concentration of 360 μM FeSO_4 induced an identical phenotypic difference. Precipitate production by the WT strain was not observed under the conditions tested. We note that iron concentration is not reported as part of the manufacturer's specifications sheet for EMJH medium.

ICP-MS was used to examine the metal and trace element isotope composition of cell pellets from cultures in which the phenotypic difference was observed. Figure 1B shows the ICP-MS spectra between 53.6 and 56.1 atomic mass units (AMU). Differences were observed in isotope Fe^{56} , with a final ion count of >2,760,000 for L522 in comparison to <50,000 measured for the parent strain. The results indicated that the precipitate produced by the mutant contained a higher concentration of iron than the parent strain precipitate. Across the spectrum, no other difference in metal ion profiles was observed.

***la4131* mutation causes surface association of precipitated iron and vesicle formation.** Iron acquisition by bacterial cells is an active process mediated by proteins in the OM. Iron precipitate production by the *la4131* mutant may affect, or be the result of, alterations in OM architecture. To determine if L522 displayed

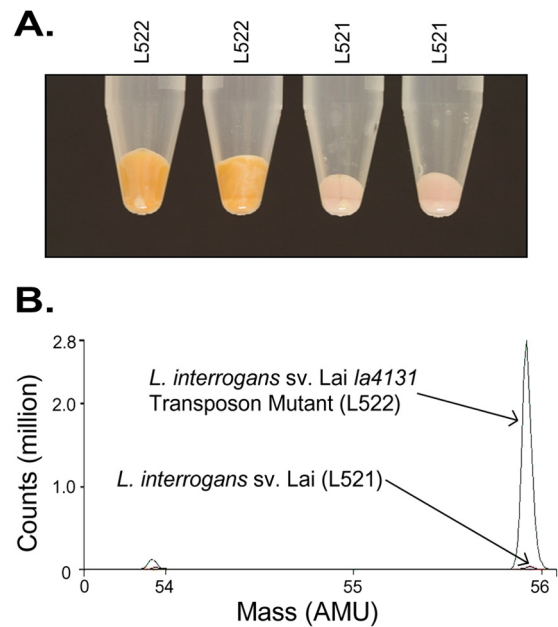


FIG 1 Iron-associated phenotypic difference between the *L. interrogans* sv Lai *la4131* mutant (L522) and the *L. interrogans* sv Lai (L521) parent strain after culture in EMJH lot 701688. Cell pellets were prepared from 5-ml cultures of L521 and L522 pelleted at $4,000 \times g$ for 5 min. (A) Overlaid mass spectra generated using inductively coupled plasma mass spectrometry (ICP-MS) conducted on pelleted samples of L522 and L521. (B) The spectra in the region of 53.6 to 56.1 atomic mass units (AMU) are shown.

altered surface characteristics, two imaging techniques, atomic force microscopy (AFM) and transmission electron microscopy (TEM), were employed.

AFM produces topographical images of bacterial cell surface structures. Highly viscous materials, such as outer membrane vesicles (OMVs), are identified as bright or illuminated features by phase-contrast AFM (51). By AFM, cells of the parental L521 strain, cultured under conditions of high or normal concentrations of iron, exhibited typical leptospiral features, such as helical morphology, periplasmic flagella, and OMVs (Fig. 2A and B). Vesicles were primarily associated with the periphery of the cell. Characterization of membranous features as OMVs was based on morphological comparison to surface structures previously observed in leptospiral TEM images (52, 53) (Fig. 2C). The mutant L522 strain cultured with normal iron concentrations displayed features similar to those observed for strain L521. In contrast, substantial differences in cell surface characteristics were observed for L522 cells cultured under conditions of high iron concentrations (Fig. 2D and E); these were associated with an array of extracellular materials (Fig. 2E). In comparison to the parent strain (Fig. 2C), L522 cells had an illuminated surface indicative of increased surface viscosity consistent with excessive membrane blebbing (Fig. 2F). Thus, the absence of a functional *la4131* gene caused an overall increase in surface viscosity and accumulation of precipitated material on the cell periphery.

TEM images of unstained L521 cells showed no electron-dense material associated with the cell irrespective of the growth medium (Fig. 3A and B). In contrast, electron-dense material was observed associated with the L522 mutant cultured under conditions of high and normal iron concentrations (Fig. 3C and D). At

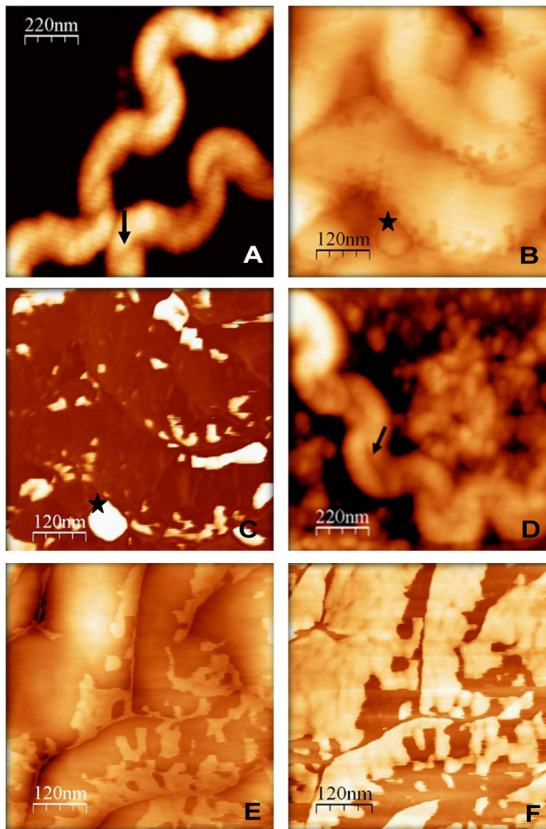


FIG 2 Micrographs generated using atomic force microscopy (AFM) showing the surface characteristics of *L. interrogans* sv Lai strain L521 (A, B, and C) and *L. interrogans* sv Lai *la4131* mutant L522 (D, E, and F). Bacteria were grown in BD EMJH lot 8170035 supplemented with 360 μM FeSO_4 . Cultures of the *la4131* mutant (D) show the presence of cell-associated material. Images were acquired in tapping (A, B, D, and E) or phase-contrast (C and F) modes. Increased viscoelasticity is shown as light coloration on phase-contrast images. Cultures of the *la4131* mutant showed overall increased surface viscosity. Stars (\star) indicate outer membrane vesicles. Arrows (\uparrow) indicate flagella. The fine white lines that occur in the AFM images are image-processing artifacts due to the line-by-line leveling process.

normal EMJH concentrations of FeSO_4 (36 μM), electron-dense material was closely associated at the junction between aggregated cells (Fig. 3C). Iron precipitates were not observed on the surface of singular separate leptospire. At high iron concentrations, there was a large increase in the amount of electron-dense material in L522 cultures (Fig. 3D). Precipitates were associated with both single and aggregated L522 cells. The production and release of OMVs from the cell surface were also increased under high iron conditions. The majority of electron-dense material was associated with the L522 cell periphery and the released OMVs. However, a proportion of the precipitate was clumped in the extracellular milieu and no longer associated with the cells, consistent with the hypothesis that mutation of *la4131* increased iron association and passive precipitation at the surface of L522.

Effect of *la4131* mutation on global gene regulation. The effect of *la4131* mutation was assessed by microarray. Mutation of *la4131* combined with growth at normal iron levels resulted in the differential expression of 11 genes (Table 2) in comparison to L521 cultured under the same conditions. Of these, the protein products of only three genes, namely, GTP pyrophosphokinase

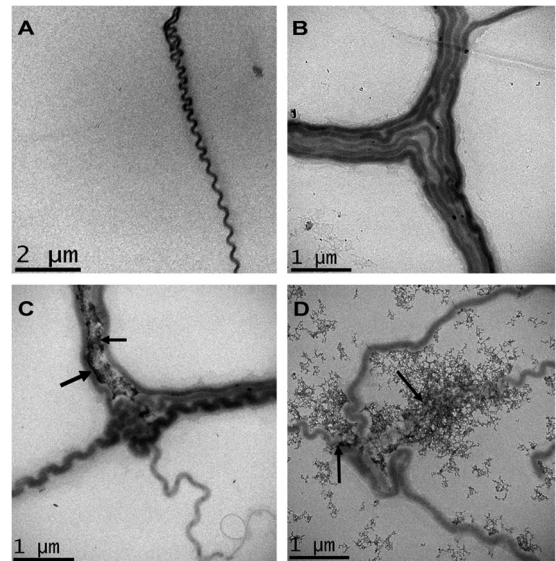


FIG 3 Transmission electron microscopy of *L. interrogans* strain L521 (A and B) and *L. interrogans* sv Lai *la4131* mutant L522 (C and D) cultured in EMJH medium or EMJH medium supplemented with 360 μM FeSO_4 . The bacteria were grown in BD EMJH lot 8170035 (A and C) and BD EMJH lot 8170035 supplemented with 360 μM FeSO_4 (B and D). Arrows indicate accumulated electron-dense material.

SpoT (LA3085), leptospiral endostatin-like protein LenD (LA1433; binds to laminin and fibronectin of host organisms [54]), and a methyl-accepting chemotaxis protein (MCP) (SPN3218), had known or predicted functions.

Comparison of the mutant strain, L522, to the parent strain, L521, in the presence of increased FeSO_4 identified 13 differentially expressed genes. Of these genes, the protein products of five were orthologous to those of known bacterial cellular stress response genes (Table 2) (55–59). Comparison of levels of gene expression in the L522 mutant grown under normal and high iron conditions identified 19 differentially expressed genes; 10 of these genes had annotated functions (Table 2). The same comparison performed with the parental L521 strain showed reduced expression for *la3778*, *la1027*, and *la2200*; these same three genes followed the same pattern of expression in the L522 mutant strain. These genes encode potential virulence factors, LigB (*la3778*), sphingomyelinase C (*la1027*), and a putative amidase (*la2200*). Thus, the differential expression of these genes is related to iron concentration and is independent of the *la4131* mutation.

DISCUSSION

This study has investigated a transposon mutant of a putative HtpX-like metalloprotease, LA4131, and examined the phenotypic alterations associated with *in vitro* iron concentrations. Sequence similarity analysis demonstrated that LA4131 is most related to the M48 family of metalloproteases. M48 metalloproteases share similarity with heat shock proteins, such as *E. coli* HtpX and *Saccharomyces cerevisiae* Ste24p. These heat shock proteins respond to changes in temperature, exposure to UV irradiation, bacteriophage infection, and the presence of accumulated misfolded proteins (60–65). The proposed role of M48 metalloproteases is in the degradation of misfolded intracellular proteins (21, 28, 31, 62).

Genes encoding protein orthologs of the HtpX-like metallo-

TABLE 2 Comparison of global gene expression characteristics of strains L521 and L522

Strain comparison and locus tag	Fold difference ^a	Gene	Gene product	Location ^b	COG ^c
L522 vs L521—both normal iron					
LA2066	-6.5		Hypothetical protein		
LA3085	-6.3	<i>spoT</i>	GTP pyrophosphokinase	Cyt	T, K
LA2065	-3.9		Hypothetical protein	Cyt	
LA2013	-3.8		Hypothetical protein		
LA2020	-3.0		Hypothetical protein		
LA1762	-2.3		Hypothetical lipoprotein	OM	
LA1433	-2.2	<i>lenD</i>	Leptospiral endostatin-like protein, LenD	OM	
LA1761	-2.0		Hypothetical lipoprotein		
LA3145	+2.0		Hypothetical protein		S
LA0598	+2.1		Hypothetical protein		S
SPN3218	+2.3		Methyl-accepting chemotaxis protein	CM	N, T
L522 vs L521—both high iron					
LA2065	-5.5		Hypothetical protein	Cyt	
LA2066	-5.4		Hypothetical protein		
LA1844	-2.1		Hypothetical protein		
LA0189	+2.1		Mu-like bacteriophage protein	Cyt	R
LA0802	+2.1		TPR repeat-containing protein		N, U
LA3145	+2.2		Hypothetical protein		S
LA3926	+2.3		AcrB family efflux pump	CM	V
LA1369	+2.4		Hypothetical protein		
LA2110	+2.4	<i>bolA</i>	Putative transcriptional regulator, BolA	Cyt	T
LA3018	+2.5		Hypothetical protein	CM	R
LA1879	+2.5	<i>clpB</i>	Endopeptidase ClpB	Cyt	O
LA0593	+4.0	<i>copZ</i>	Copper chaperone	Cyt	P
LA1124	+6.1	<i>lnt-1</i>	Apolipoprotein N-acyltransferase	CM	M
L522 normal iron vs L522 high iron					
LA0634	-5.7		Putative permease	CM	E, P
LA3781	-2.7		Hypothetical lipoprotein		
LA3780	-2.5		Hypothetical lipoprotein		
LA4128	-2.5		Hypothetical protein		
LA3778	-2.3	<i>ligB</i>	LigB lipoprotein		N
LA1072	-2.3		D-Alanine D-alanine ligase		H, J
LA1027	-2.1		Sphingomyelinase C precursor	OM	R
LIC12947	-2.1		Putative endoflagellum-like protein		N
LA2200	-2.1		Putative amidase		M
LB105	-2.0		Putative methyltransferase		
LB107	-2.0		Putative ferredoxin		C
LA0863	+2.0		Putative acetolactate synthase		E, H
LA0212	+2.2		Hypothetical protein		
LA_SPN1928	+2.4		Hypothetical lipoprotein		
LA0593	+2.7	<i>copZ</i>	Copper chaperone	Cyt	P
LA3018	+2.8		Hypothetical protein	CM	R
LA0980	+3.5	<i>thiC</i>	Thiamine biosynthesis protein, ThiC	Cyt	H
LA3017	+3.8		Hypothetical lipoprotein		S
LA3016	+4.1		Hypothetical protein		
L521 normal iron vs L521 high iron					
LA2200	-3.1		Putative amidase		M
LA0101	-2.8		Hypothetical protein		
LA3781	-2.5		Hypothetical lipoprotein		
LA3778	-2.5	<i>ligB</i>	LigB lipoprotein		N
LA0815	-2.3		Signal transduction histidine kinase	CM	T
LA0100	-2.2		Hypothetical protein	CM	
LA1027	-2.1		Sphingomyelinase C precursor	OM	R
LA_SPN1928	+2.1		Hypothetical lipoprotein		
LA1468	+2.5		Hypothetical lipoprotein	CM	

^a Differentially expressed genes have at least a 2-fold difference in gene expression at a confidence level of 95%.

^b Cellular localization predicted using PSORTB. Localization abbreviations: Cyt, cytoplasmic; CM, cytoplasmic membrane; Per, periplasmic; OM, outer membrane; Ext, extracellular.

^c Cluster of orthologous group (COG) categories (79). COG categories were as follows: cellular processing and signaling (COGs D, Y, V, M, T, N, Z, W, U, and O), metabolism (COGs C, G, E, F, H, I, P, and Q), information storage (COGs J, A, K, L, and B), and processing or poorly characterized (COGs R and S).

protease LA4131 were identified within the available sequenced genomes of pathogenic leptospires, with the exception of the bovine pathogen *L. borgpetersenii*. It has been suggested that *L. borgpetersenii* is undergoing a process of genome reduction (66) centered on the inactivation of genes associated with environmental sensing, metabolite transport, and utilization. It can thus be hypothesized that the absence of a LA4131 ortholog, a protein with a putative role in environmental stress response, is a direct result of these processes. The ortholog identified within the saprophyte *L. biflexa* shares 28% similarity with LA4131. However, based on protein topology, the saprophytic protein is more similar to classical HtpX metalloprotease than that of LA4131, suggesting that LA4131 may play a unique but related function within pathogenic leptospires.

The N-terminal signal peptide is essential for protein translocation and localization of the *E. coli* M48 metalloprotease, HtpX, to the inner membrane (IM) (21). Characterized HtpX proteins have two to four transmembrane helices that aid integration into the IM after protein translocation (21, 22, 28). Despite regions of local similarity to the *E. coli* HtpX, it is apparent that the leptospiral LA4131 has a different membrane topology. LA4131 contains an N-terminal signal peptide, but the presence of small hydrophobic residues preceding the predicted signal peptidase I cleavage site indicates that this protein may be translocated across the IM by SecII-dependent processes and targeted to the OM. Supporting this notion, and in contrast to the *E. coli* HtpX, LA4131 has no predicted transmembrane helices but rather predicted C-terminal β -structures, consistent with localization in the OM. The OM localization is further supported by the MudPit analysis by Lo et al. (67) that found LA4131 located exclusively in the TX-114 extracted OM fractions from *L. interrogans*. Combined, our data suggest that LA4131 is different from other M48 metalloproteases in that LA4131 is the first to have a predicted OM localization.

Generally, M48 metalloproteases have roles in the maintenance of membrane homeostasis, specifically in the removal of misfolded, nonfunctional proteins. Thus, phenotypic changes are likely to be indirect and due to interruption of normal membrane operation. Under high iron conditions, mutational inactivation of *la4131* resulted in a phenotype where precipitated iron was associated with the bacterial surface along with the production of OM blebs and the subsequent release of outer membrane vesicles (OMVs). Thus, it is hypothesized that membrane-associated proteins, used in the management of excessive environmental iron concentrations, were not able to function normally in the LA4131 mutant due to the absence of a functional M48 metalloprotease to enable the appropriate reconfiguration of the membrane, resulting in OMV formation. This leads to the suggestion that M48 metalloproteases may play a role in facilitating the rapid retooling of membranes to suit prevailing environmental conditions.

The control of the intracellular iron concentration at below toxic levels is essential for life. The phenotype observed in the mutant is indicative of the mechanism used to maintain intracellular iron below toxic concentrations. In the LA4131 mutant, under high iron conditions, an alternative passive mechanism for management of intracellular iron concentrations is activated.

Examination of the passive management of iron concentration observed in the LA4131 mutant suggested that the destabilization of the OM and the sloughing of OMVs are likely to be part of a more generalized mechanism used by bacteria to manage intracel-

lular toxicity. Vesiculation can function as part of cellular stress response system by aiding bacterial survival through specific enrichment and release of toxic compounds from the cell (2, 9, 68–70). However, the mechanism of OMV formation and release is not well characterized. McBroom and Kuehn (10) investigated defined mutants of *E. coli* Cpx and σ^F stress response pathway proteins and found a positive correlation between vesicle production, intracellular concentration of accumulated misfolded proteins, and the impairment of stress response mechanisms. Our report furthers this work and is the first to demonstrate a correlation between vesicle production and accumulation of surface iron due to the impairment of the activity of the LA4131 metalloprotease.

Transcription analysis allowed us to hypothesize a molecular basis for the phenotype observed in the LA4131 mutant. The reduced expression of the transcriptional regulator *spoT* (*la3085*), which is upregulated under conditions of iron limitation (71), is consistent with an oversupply of iron. There is enhanced transcription of cell homeostasis and stress response genes, such as that encoding the methyl-accepting chemotaxis protein (MCP), *SPN3218*. Expression of MCPs enables bacteria to detect extracellular repellents or attractants, alter motility gene expression, and thus move toward a more favorable environment (72), such as in this case, perhaps facilitating migration toward a lower iron concentration.

The enhanced expression of membrane oxidative stress response genes *bolA* and *clpB* (58, 73) in conjunction with *hnt-1* may directly enhance OMV formation (10). The production of vesicles would result in an overall reduction of the surface iron concentration (9), which in turn would alleviate some of the associated intracellular iron toxicity. Furthermore, upregulation of the expression of *copZ* and *thiC* with a concomitant reduction in *la0634*, encoding a putative metal transport protein, may aid in further limiting the heavy metal toxicity and promote cell survival (74–76).

LA4131 is a member of the HtpX metalloprotease family of stress response proteins. We suggest that this protein has a cellular location in the OM that sets it apart from other members of this family of proteins, although its cellular role is likely to be similar to that of other M48 metalloproteases. This investigation of LA4131 under high iron conditions highlights the complexity of bacterial stress response pathways and their ability to compensate for loss of the activity of one of their component proteins in order to enable survival.

ACKNOWLEDGMENTS

This work was supported by the National Health and Medical Research Council and the Australian Research Council, Canberra, Australia, and in part by the Commonwealth of Australia under the International Science Linkages program and is related to the Australian-European integrated FP6 CHARPAN and FP7 BISNES projects.

REFERENCES

1. Lovely DR. 2000. Fe(III) and Mn(IV) reduction, p 3–30. In Lovely DR (ed), Environmental microbe-metal interactions. ASM Press, Washington, DC.
2. Beveridge TJ. 1989. Role of cellular design in bacterial metal accumulation and mineralization. Annu. Rev. Microbiol. 43:147–171.
3. Southam G. 2000. Bacterial surface-mediated mineral formation, p 257–276. In Lovely DR (ed), Environmental microbe-metal interactions. ASM Press, Washington DC.
4. Chatellier X, Fortin D, West MM, Leppard GG, Ferris FG. 2001. Effect

- of the presence of bacterial surfaces during the synthesis of Fe oxides by oxidation of ferrous ions. *Eur. J. Mineral.* 13:705–714.
5. Fortin D, Langley S. 2005. Formation and occurrence of biogenic iron-rich minerals. *Earth Sci. Rev.* 72:1–19.
 6. Frankel RB, Bazylinski DA. 2003. Biologically induced mineralization by bacteria. *Rev. Mineral Geochem.* 54:95–114.
 7. Suzuki T, Hashimoto H, Ishihara H, Kasai T, Kunoh H, Takada J. 2011. Structural and spatial associations between Fe, O, and C in the network structure of the *Leptothrix ochracea* sheath surface. *Appl. Environ. Microbiol.* 77:7873–7875.
 8. Schwachheimer C, Sullivan CJ, Kuehn MJ. 2013. Envelope control of outer membrane vesicle production in gram-negative bacteria. *Biochemistry* 52:3031–3040.
 9. Macdonald IA, Kuehn MJ. 2012. Offense and defense: microbial membrane vesicles play both ways. *Res. Microbiol.* 163:607–618.
 10. McBroom AJ, Kuehn MJ. 2007. Release of outer membrane vesicles by Gram-negative bacteria is a novel envelope stress response. *Mol. Microbiol.* 63:545–558.
 11. McBroom AJ, Johnson AP, Vemulapalli S, Kuehn MJ. 2006. Outer membrane vesicle production by *Escherichia coli* is independent of membrane instability. *J. Bacteriol.* 188:5385–5392.
 12. Song T, Mika F, Lindmark B, Liu Z, Schild S, Bishop A, Zhu J, Camilli A, Johansson J, Vogel J, Wai SN. 2008. A new *Vibrio cholerae* sRNA modulates colonization and affects release of outer membrane vesicles. *Mol. Microbiol.* 70:100–111.
 13. Berlanda Scorza F, Doro F, Rodriguez-Ortega MJ, Stella M, Liberatori S, Taddei AR, Serino L, Gomes Moriel D, Nesta B, Fontana MR, Spagnuolo A, Pizza M, Norais N, Grandi G. 2008. Proteomics characterization of outer membrane vesicles from the extraintestinal pathogenic *Escherichia coli* DeltatolR IHE3034 mutant. *Mol. Cell. Proteomics* 7:473–485.
 14. Lee EY, Bang JY, Park GW, Choi DS, Kang JS, Kim HJ, Park KS, Lee JO, Kim YK, Kwon KH, Kim KP, Cho YS. 2007. Global proteomic profiling of native outer membrane vesicles derived from *Escherichia coli*. *Proteomics* 7:3143–3153.
 15. Iwami J, Murakami Y, Nagano K, Nakamura H, Yoshimura F. 2007. Further evidence that major outer membrane proteins homologous to OmpA in *Porphyromonas gingivalis* stabilize bacterial cells. *Oral Microbiol. Immunol.* 22:356–360.
 16. Button JE, Silhavy TJ, Ruiz N. 2007. A suppressor of cell death caused by the loss of sigmaE downregulates extracytoplasmic stress responses and outer membrane vesicle production in *Escherichia coli*. *J. Bacteriol.* 189:1523–1530.
 17. Alaniz RC, Deatherage BL, Lara JC, Cookson BT. 2007. Membrane vesicles are immunogenic facsimiles of *Salmonella typhimurium* that potentially activate dendritic cells, prime B and T cell responses, and stimulate protective immunity in vivo. *J. Immunol.* 179:7692–7701.
 18. Giuliodori AM, Gualerzi CO, Soto S, Vila J, Tavio MM. 2007. Review on bacterial stress topics. *Ann. N. Y. Acad. Sci.* 1113:95–104.
 19. Barchinger SE, Ades SE. 2013. Regulated proteolysis: control of the *Escherichia coli* sigma(E)-dependent cell envelope stress response. *Subcell. Biochem.* 66:129–160.
 20. Dorel C, Lejeune P, Rodrigue A. 2006. The Cpx system of *Escherichia coli*, a strategic signaling pathway for confronting adverse conditions and for settling biofilm communities? *Res. Microbiol.* 157:306–314.
 21. Shimohata N, Chiba S, Saikawa N, Ito K, Akiyama Y. 2002. The Cpx stress response system of *Escherichia coli* senses plasma membrane proteins and controls HtpX, a membrane protease with a cytosolic active site. *Genes Cells* 7:653–662.
 22. Huang Y, Zhang B, Dong K, Zhang X, Hou L, Wang T, Chen N, Chen S. 2007. Up-regulation of *yggG* promotes the survival of *Escherichia coli* cells containing Era-1 mutant protein. *FEMS Microbiol. Lett.* 275:8–15.
 23. Lüdke A, Kramer R, Burkovski A, Schluesener D, Poetsch A. 2007. A proteomic study of *Corynebacterium glutamicum* AAA+ protease FtsH. *BMC Microbiol.* 7:6. doi:10.1186/1471-2180-7-6.
 24. Kanehara K, Ito K, Akiyama Y. 2002. YaeL (EcfE) activates the sigma(E) pathway of stress response through a site-2 cleavage of anti-sigma(E), RseA. *Genes Dev.* 16:2147–2155.
 25. Alba BM, Leeds JA, Onufryk C, Lu CZ, Gross CA. 2002. DegS and YaeL participate sequentially in the cleavage of RseA to activate the sigma(E)-dependent extracytoplasmic stress response. *Genes Dev.* 16:2156–2168.
 26. McMahon KJ, Castelli ME, Garcia Vescovi E, Feldman MF. 2012. Biogenesis of outer membrane vesicles in *Serratia marcescens* is thermo-regulated and can be induced by activation of the Rcs phosphorelay system. *J. Bacteriol.* 194:3241–3249.
 27. Spiess C, Beil A, Ehrmann M. 1999. A temperature-dependent switch from chaperone to protease in a widely conserved heat shock protein. *Cell* 97:339–347.
 28. Sakoh M, Ito K, Akiyama Y. 2005. Proteolytic activity of HtpX, a membrane-bound and stress-controlled protease from *Escherichia coli*. *J. Biol. Chem.* 280:33305–33310.
 29. Akiyama Y. 2009. Quality control of cytoplasmic membrane proteins in *Escherichia coli*. *J. Biochem.* 146:449–454.
 30. Marciniak BC, Trip H, Fusetti F, Kuipers OP. 2012. Regulation of *ykrL* (*htpX*) by Rok and YkrK, a novel type of regulator in *Bacillus subtilis*. *J. Bacteriol.* 194:2837–2845.
 31. Vickerman MM, Mather NM, Minick PE, Edwards CA. 2002. Initial characterization of the *Streptococcus gordonii* *htpX* gene. *Oral Microbiol. Immunol.* 17:22–31.
 32. Gardy JL, Laird MR, Chen F, Rey S, Walsh CJ, Ester M, Brinkman FS. 2005. PSORTb v. 2.0: expanded prediction of bacterial protein subcellular localization and insights gained from comparative proteome analysis. *Bioinformatics* 21:617–623.
 33. Rey S, Acab M, Gardy JL, Laird MR, deFays K, Lambert C, Brinkman FS. 2005. PSORTdb: a protein subcellular localization database for bacteria. *Nucleic Acids Res.* 33:D164–D168.
 34. Bendtsen JD, Nielsen H, von Heijne G, Brunak S. 2004. Improved prediction of signal peptides: SignalP 3.0. *J. Mol. Biol.* 340:783–795.
 35. Juncker AS, Willenbrock H, Von Heijne G, Brunak S, Nielsen H, Krogh A. 2003. Prediction of lipoprotein signal peptides in Gram-negative bacteria. *Protein Sci.* 12:1652–1662.
 36. Setubal JC, Reis M, Matsunaga J, Haake DA. 2006. Lipoprotein computational prediction in spirochaetal genomes. *Microbiology* 152:113–121.
 37. Bendtsen JD, Jensen LJ, Blom N, Von Heijne G, Brunak S. 2004. Feature-based prediction of non-classical and leaderless protein secretion. *Protein Eng. Des. Sel.* 17:349–356.
 38. Tjalsma H. 2007. Feature-based reappraisal of the *Bacillus subtilis* exproteome. *Proteomics* 7:73–81.
 39. Arai M, Mitsuke H, Ikeda M, Xia JX, Kikuchi T, Satake M, Shimizu T. 2004. ConPred II: a consensus prediction method for obtaining transmembrane topology models with high reliability. *Nucleic Acids Res.* 32:W390–W393.
 40. Bourhy P, Louvel H, Saint Girons I, Picardeau M. 2005. Random insertional mutagenesis of *Leptospira interrogans*, the agent of leptospirosis, using a mariner transposon. *J. Bacteriol.* 187:3255–3258.
 41. Murray GL, Ellis KM, Lo M, Adler B. 2008. *Leptospira interrogans* requires a functional heme oxygenase to scavenge iron from hemoglobin. *Microbes Infect.* 10:791–797.
 42. PerkinElmer. 2011. The 30-minute guide to ICP-MS. http://www.perkinelmer.com/CMSResources/Images/44-74849tch_icpmsthirtyminuteguide.pdf.
 43. Dauphas N, Rouxel O. 2006. Mass spectrometry and natural variations of iron isotopes. *Mass Spectrom. Rev.* 25:515–550.
 44. Balcia N, Bullenb TD, Witte-Lienc K, Shanksd WC, Motelicae M, Mandernacka KW. 2006. Iron isotope fractionation during microbially stimulated Fe(II) oxidation and Fe(III) precipitation. *Geochim. Cosmochim. Acta* 70:622–639.
 45. Lo M, Bulach DM, Powell DR, Haake DA, Matsunaga J, Paustian ML, Zuerner RL, Adler B. 2006. Effects of temperature on gene expression patterns in *Leptospira interrogans* serovar Lai as assessed by whole-genome microarrays. *Infect. Immun.* 74:5848–5859.
 46. Reference deleted.
 47. Nascimento AL, Verjovski-Almeida S, Van Sluys MA, Monteiro-Vitorello CB, Camargo LE, Digiampietri LA, Harstkeerl RA, Ho PL, Marques MV, Oliveira MC, Setubal JC, Haake DA, Martins EA. 2004. Genome features of *Leptospira interrogans* serovar Copenhageni. *Braz. J. Med. Biol. Res.* 37:459–477.
 48. Ren SX, Fu G, Jiang XG, Zeng R, Miao YG, Xu H, Zhang YX, Xiong H, Lu G, Lu LF, Jiang HQ, Jia J, Tu YF, Jiang JX, Gu WY, Zhang YQ, Cai Z, Sheng HH, Yin HF, Zhang Y, Zhu GF, Wan M, Huang HL, Qian Z, Wang SY, Ma W, Yao ZJ, Shen Y, Qiang BQ, Xia QC, Guo XK, Danchin A, Saint Girons I, Somerville RL, Wen YM, Shi MH, Chen Z, Xu JG, Zhao GP. 2003. Unique physiological and pathogenic features of *Leptospira interrogans* revealed by whole-genome sequencing. *Nature* 422:888–893.

49. Ricaldi JN, Fouts DE, Selengut JD, Harkins DM, Patra KP, Moreno A, Lehmann JS, Purushe J, Sanka R, Torres M, Webster NJ, Vinetz JM, Matthias MA. 2012. Whole genome analysis of *Leptospira licerasiae* provides insight into leptospiral evolution and pathogenicity. *PLoS Negl. Trop. Dis.* 6:e1853. doi:10.1371/journal.pntd.0001853.
50. Bagos PG, Liakopoulos TD, Spyropoulos IC, Hamodrakas SJ. 2004. A Hidden Markov Model method, capable of predicting and discriminating beta-barrel outer membrane proteins. *BMC Bioinformatics* 5:29. doi:10.1186/1471-2105-5-29.
51. Stukalov O, Korenevsky A, Beveridge TJ, Dutcher JR. 2008. Use of atomic force microscopy and transmission electron microscopy for correlative studies of bacterial capsules. *Appl. Environ. Microbiol.* 74:5457–5465.
52. Ritchie AE, Ellinghausen HC. 1965. Electron microscopy of leptospires. I. Anatomical features of *Leptospira* Pomona. *J. Bacteriol.* 89:223–233.
53. Anderson DL, Johnson RC. 1968. Electron microscopy of immune disruption of leptospires: action of complement and lysozyme. *J. Bacteriol.* 95:2293–2309.
54. Stevenson B, Choy HA, Pinne M, Rotondi ML, Miller MC, Demoll E, Kraiczy P, Cooley AE, Creamer TP, Suchard MA, Brissette CA, Verma A, Haake DA. 2007. *Leptospira interrogans* endostatin-like outer membrane proteins bind host fibronectin, laminin and regulators of complement. *PLoS One* 2:e1188. doi:10.1371/journal.pone.0001188.
55. Peeters E, Sass A, Mahenthiralingam E, Nelis H, Coenye T. 2010. Transcriptional response of *Burkholderia cenocepacia* J2315 sessile cells to treatments with high doses of hydrogen peroxide and sodium hypochlorite. *BMC Genomics* 11:90. doi:10.1186/1471-2164-11-90.
56. Ma D, Cook DN, Alberti M, Pon NG, Nikaido H, Hearst JE. 1995. Genes *acrA* and *acrB* encode a stress-induced efflux system of *Escherichia coli*. *Mol. Microbiol.* 16:45–55.
57. Santos JM, Freire P, Vicente M, Arraiano CM. 1999. The stationary-phase morphogene *bolA* from *Escherichia coli* is induced by stress during early stages of growth. *Mol. Microbiol.* 32:789–798.
58. Lourdault K, Cerqueira GM, Wunder EA, Jr, Picardeau M. 2011. Inactivation of *clpB* in the pathogen *Leptospira interrogans* reduces virulence and resistance to stress conditions. *Infect. Immun.* 79:3711–3717.
59. Capestany CA, Tribble GD, Maeda K, Demuth DR, Lamont RJ. 2008. Role of the Clp system in stress tolerance, biofilm formation, and intracellular invasion in *Porphyromonas gingivalis*. *J. Bacteriol.* 190:1436–1446.
60. Heusipp G, Nelson KM, Schmidt MA, Miller VL. 2004. Regulation of *htrA* expression in *Yersinia enterocolitica*. *FEMS Microbiol. Lett.* 231:227–235.
61. Johnstone DB, Farr SB. 1991. AppppA binds to several proteins in *Escherichia coli*, including the heat shock and oxidative stress proteins DnaK, GroEL, E89, C45 and C40. *EMBO J.* 10:3897–3904.
62. Kornitzer D, Teff D, Altuvia S, Oppenheim AB. 1991. Isolation, characterization, and sequence of an *Escherichia coli* heat shock gene, *htpX*. *J. Bacteriol.* 173:2944–2953.
63. Mogensen JE, Kleinschmidt JH, Schmidt MA, Otzen DE. 2005. Misfolding of a bacterial autotransporter. *Protein Sci.* 14:2814–2827.
64. Ohnishi K, Matsumoto H, Takahashi A, Wang X, Ohnishi T. 1996. Heat shock transcription factor, HSF, is activated by ultraviolet irradiation. *Photochem. Photobiol.* 64:949–952.
65. Raivio TL, Silhavy TJ. 2001. Periplasmic stress and ECF sigma factors. *Annu. Rev. Microbiol.* 55:591–624.
66. Bulach DM, Zuerner RL, Wilson P, Seemann T, McGrath A, Cullen PA, Davis J, Johnson M, Kuczek E, Alt DP, Peterson-Burch B, Coppel RL, Rood JJ, Davies JK, Adler B. 2006. Genome reduction in *Leptospira borgpetersenii* reflects limited transmission potential. *Proc. Natl. Acad. Sci. U. S. A.* 103:14560–14565.
67. Lo M, Cordwell SJ, Bulach DM, Adler B. 2009. Comparative transcriptional and translational analysis of leptospiral outer membrane protein expression in response to temperature. *PLoS Negl. Trop. Dis.* 3:e560. doi:10.1371/journal.pntd.0000560.
68. Kobayashi H, Uematsu K, Hirayama H, Horikoshi K. 2000. Novel toluene elimination system in a toluene-tolerant microorganism. *J. Bacteriol.* 182:6451–6455.
69. Kuehn MJ, Kesty NC. 2005. Bacterial outer membrane vesicles and the host-pathogen interaction. *Genes Dev.* 19:2645–2655.
70. McGrath H, Adler B, Vinh T, Faine S. 1984. Phagocytosis of virulent and avirulent leptospires by guinea-pig and human polymorphonuclear leukocytes *in vitro*. *Pathology* 16:243–249.
71. Atkinson GC, Tenson T, Haurlyuk V. 2011. The RelA/SpoT homolog (RSH) superfamily: distribution and functional evolution of ppGpp synthetases and hydrolases across the tree of life. *PLoS One* 6:e23479. doi:10.1371/journal.pone.0023479.
72. Schweinitzer T, Josenhans C. 2010. Bacterial energy taxis: a global strategy? *Arch. Microbiol.* 192:507–520.
73. Moreira RN, Dressaire C, Domingues S, Arraiano CM. 2011. A new target for an old regulator: H-NS represses transcription of *bolA* morphogene by direct binding to both promoters. *Biochem. Biophys. Res. Commun.* 411:50–55.
74. Magnani D, Solioz M. 2005. Copper chaperone cycling and degradation in the regulation of the cop operon of *Enterococcus hirae*. *Biomaterials* 18:407–412.
75. Silver S, Phung LT. 2005. A bacterial view of the periodic table: genes and proteins for toxic inorganic ions. *J. Ind. Microbiol. Biotechnol.* 32:587–605.
76. Thorgersen MP, Downs DM. 2009. Oxidative stress and disruption of labile iron generate specific auxotrophic requirements in *Salmonella enterica*. *Microbiology* 155:295–304.
77. Murray GL, Morel V, Cerqueira GM, Croda J, Srikram A, Henry R, Ko AI, Dellagostin OA, Bulach DM, Sermswan RW, Adler B, Picardeau M. 2009. Genome-wide transposon mutagenesis in pathogenic *Leptospira* species. *Infect. Immun.* 77:810–816.
78. Picardeau M, Bulach DM, Bouchier C, Zuerner RL, Zidane N, Wilson PJ, Creno S, Kuczek ES, Bommezzadri S, Davis JC, McGrath A, Johnson MJ, Boursaux-Eude C, Seemann T, Rouy Z, Coppel RL, Rood JJ, Lajus A, Davies JK, Medigue C, Adler B. 2008. Genome sequence of the saprophyte *Leptospira biflexa* provides insights into the evolution of *Leptospira* and the pathogenesis of leptospirosis. *PLoS One* 3:e1607. doi:10.1371/journal.pone.0001607.
79. Tatusov RL, Koonin EV, Lipman DJ. 1997. A genomic perspective on protein families. *Science* 278:631–637.